

# Composite right/left-handed metamaterial resonant antennas

A. B. OCHETAN\*, M. G. BANCIU<sup>a</sup>, G. LOJEWSKI

*Electronics, Telecommunications and Information Technology Faculty, University Politehnica of Bucharest, 1-3 Iuliu Maniu, Bucharest, 061071, Romania*

<sup>a</sup>*National Institute of Materials Physics, 105 Atomistilor, Magurele, 077125, Romania*

By taking advantage of the unique and unusual properties of the recent composite right/left-handed metamaterial transmission line, we have designed a shunt mode resonant antenna with a multi-band operation, and a series mode zero order resonant antenna, which is frequency independent. The antennas are well matched to the external network by using compact matching circuits. The resulting radiation characteristics make these antennas suitable for short-range wireless communications systems.

(Received September 8, 2011; accepted October 20, 2011)

*Keywords:* Metamaterials, Antennas

## 1. Introduction

Left-handed metamaterials (LH MTM) are defined as artificial, effectively homogeneous electromagnetic structures not readily available in nature, with unusual properties such as backward wave propagation, negative refractive index, positive, negative and zero order resonances [1].

The Composite Right-/Left-Handed Transmission Line (CRLH TL) is a practical implementation of a LH MTM, which also includes unavoidable right-handed (RH) effects. The cell size of the CRLH TL should be at least smaller than a quarter of wavelength to ensure that the TL is an effective homogeneous structure. If the CRLH TL is terminated with an open-end or a short-end, it becomes a resonator. It can achieve multiple resonances which can be exploited in the design of multi-band [2], [3] and miniaturized antennas [4], [5] suitable for modern wireless communication systems. CRLH TLs have been also used to build microwave devices with improved performances such as leaky-wave antennas [6], directional couplers [7], power dividers [8], diplexers [9], negative group delay circuits [10] and so on.

The open-ended (shunt mode) resonant antenna has a very high input impedance. Therefore, its matching to a common microwave system is an important issue that must be solved. In this case, the matching in the close vicinity of the resonant frequencies will be achieved by using a compact series inductor. On the other hand, in the vicinity of the zero order resonant frequency, the short-circuited (series mode) resonant antenna has a very low and slowly varying input impedance. This type of antenna can be matched to the external network by using conventional matching circuits such as the parallel stub or the impedance transformer [11]. The problem with these circuits is that their sizes depend of frequency and can be quite large as

compared to the zero order resonant antenna (ZORA). As it will be shown in the following sections, by using the filter theory we will derive a miniaturized, frequency independent circuit which assures good matching results.

## 2. The shunt mode CRLH resonant antenna

Fig. 1 presents the proposed CRLH TL composed of five identical cells and terminated by an open-end. The operating wave is a standing wave and the radiation produced is based on the resonance mechanism. The structure is designed in microstrip technology, the metallization being cooper of  $17\ \mu\text{m}$  thickness and the dielectric layer being Rogers RT5880, with dielectric constant  $\epsilon_r = 2.2$  and  $1.574\ \text{mm}$  thickness. Each cell is composed of an interdigital capacitor which provides the series LH capacitance CL and a short-circuited stub which provides the parallel LH inductance LL. When characterizing the cell, the effects of parasitic RH elements (LR and CR) must be taken into account. This is shown in Fig. 1, where the cell's equivalent circuit is also presented.

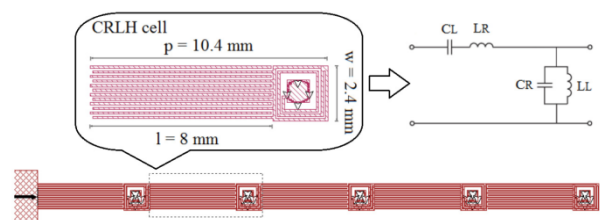


Fig. 1. The proposed shunt mode structure and the cell's equivalent circuit

For regular open-ended RH resonators, the resonances

are achieved when the physical length of the structure is equal to a multiple of half a wavelength or when the electrical length ( $\theta_m$ ) is a multiple of  $\pi$ . This is expressed by (1).

$$\theta_m = \beta \cdot l = \frac{2\pi}{\lambda} \cdot \frac{m\lambda}{2} = m\pi, \quad (1)$$

where  $l$  is the length of the structure.

For the RH structure, its phase constant ( $\beta$ ) is positive and linear and therefore the resonance frequencies are positive and in harmonic ratios. In the case of CRLH structure, its phase constant can be determined with (2) and, as shown in Fig. 2, it can be positive, negative or even equal to zero. By sampling the CRLH structure's dispersion diagram with  $m\pi/l$  ( $m=\{0, \pm 1, \pm 2, \dots\}$ ) we obtain the positive order, the negative order resonances and also a zero order resonance. The structure can be considered effectively homogeneous only for the first  $N-1$  positive and negative resonance frequencies,  $N$  being the number of constitutive cells.

$$\beta = -\phi^{\text{unwrapped}}(S_{21})/l, \quad (2)$$

where  $\phi^{\text{unwrapped}}(S_{21})$  is the unwrapped transmission phase of the CRLH structure, obtained using electromagnetic simulations based of method of moments [12].

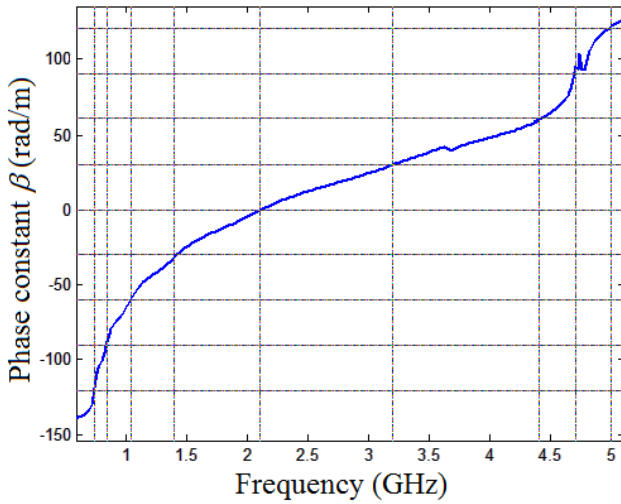


Fig. 2. Sampled CRLH structure's dispersion diagram. The grid lines indicate the resonance frequencies as in Table I.

The resonance frequencies of the structure from Fig. 1 are presented in Table I. They are not in harmonic ratios and have been designed by exploiting the dispersion diagram which can be tailored by modifying the cell's LC elements. The zero order resonance ( $m = 0$ ) is of great interest due to the fact that it corresponds to the transition frequency where  $\beta = 0$  and therefore its frequency does not depend on the physical length of the resonator. This means that the zero order resonance has a huge potential for antenna miniaturization.

Table I. Resonance frequencies

Order	Frequency (GHz)
$m = -4$	0.74
$m = -3$	0.84
$m = -2$	1.04
$m = -1$	1.4
$m = 0$	2.1
$m = +1$	3.2
$m = +2$	4.4
$m = +3$	4.7
$m = +4$	5

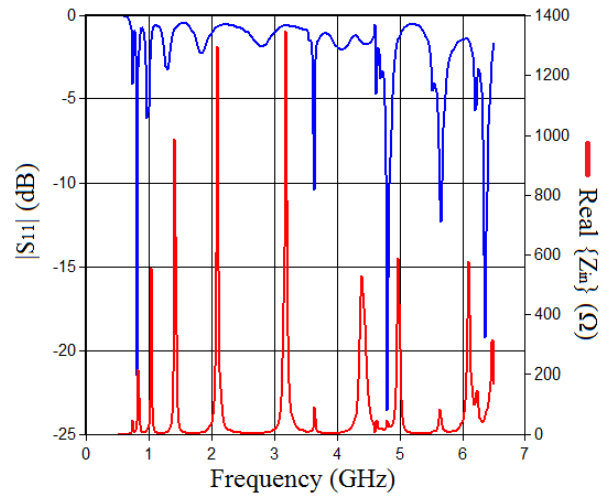


Fig. 3. Magnitude of reflection coefficient and real part of input impedance.

Fig. 3 shows the magnitude of the reflection coefficient of the CRLH structure from Fig. 1, excited at one of its ends. At the resonance frequencies the input impedance of the CRLH structure is very high, leading to a mismatch problem and consequently to a low efficiency.

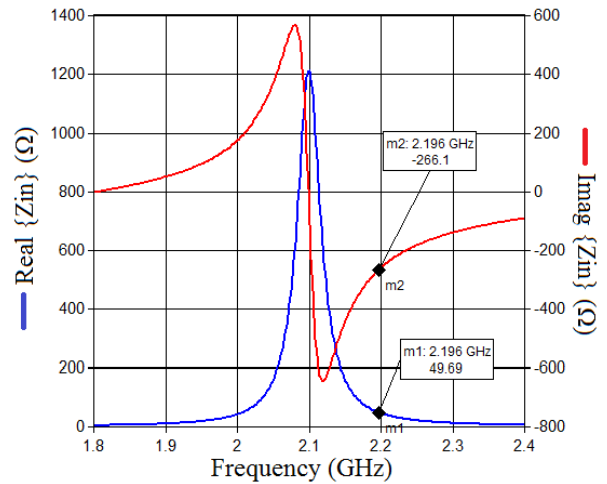


Fig. 4. Input impedance versus frequency for the zero order resonance

As shown in Fig. 4, in the close vicinity of the zero

order resonance ( $f_0 = 2.1$  GHz), the real part of the input impedance drops fast to the  $50 \Omega$  value and therefore the matching problem can be solved if the reactive part is cancelled. This can be done by adding a series inductor as shown in Fig. 5, designed with (3) [13] for a specific inductance. This inductance should also compensate the series capacitance that appears from the meander configuration of the inductor.



Fig. 5. CRLH resonant antenna with matching circuit

$$L = \frac{\mu_0 t}{4\pi} \left[ 2a \sinh\left(\frac{t}{w}\right) + 2\left(\frac{t}{w}\right) \cdot a \sinh\left(\frac{w}{t}\right) - \frac{2(w^2 + t^2)^{3/2}}{3t \cdot w^2} + \frac{2}{3}\left(\frac{t}{w}\right)^2 + \frac{2w}{3t} \right], \quad (3)$$

where  $t$  is the length and  $w$  is the width of the strip inductor.

As shown in Fig. 6, by using the series inductor, the matching is significantly improved at the zero order resonance  $f_0 = 2.1$  GHz, but also in the vicinity of the first negative ( $f_{-1}$ ) and of the first positive ( $f_{+1}$ ) resonant frequency.

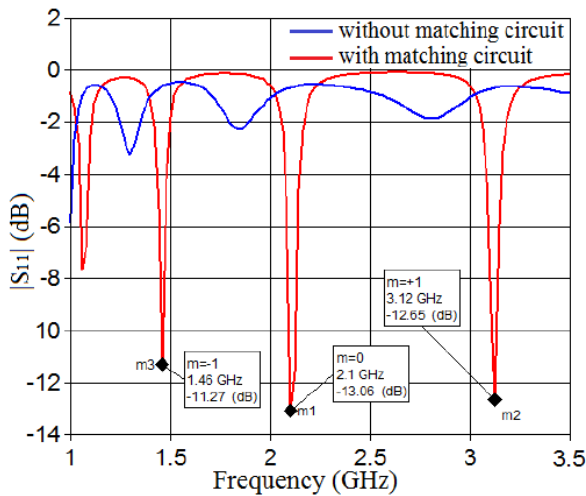


Fig. 6. Magnitude of reflection coefficient.

Fig. 7 presents the surface current density for the zero order resonance. It shows high and constant values inside the short-circuited inductors and very low values in the interdigital capacitors. Due to this constant distribution the field will be in-phase, with equal amplitude, in all points along the structure's length, as shown in Fig. 8. Consequently the equivalent magnetic current density [14], determined with (4), will create a loop, as shown in Fig. 9 (a).

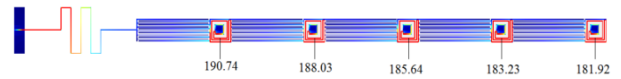


Fig. 7. Simulated surface current density for  $f_0$ . The values are in A/m and the cold colours correspond to low values.

$$\vec{M}_S = -2\vec{n} \times \vec{E}, \quad (4)$$

where  $\vec{n}$  is the unit normal to the edge and  $\vec{E}$  is the electric field. This magnetic loop corresponds to an ideal electric dipole and produces a monopole radiation pattern [15], as demonstrated in Fig. 10.

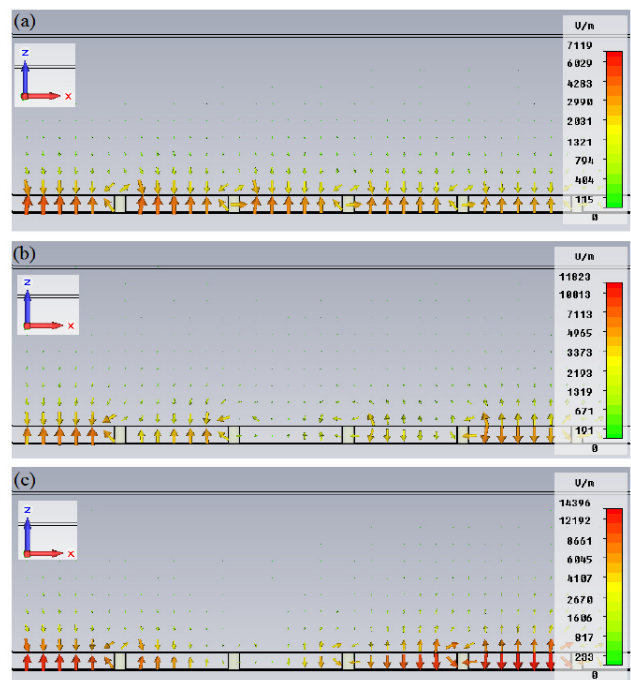


Fig. 8. Electric field distribution along the length of the CRLH resonant antenna obtained using electromagnetic simulations [16] at: (a)  $f_0 = 2.1$  GHz, (b)  $f_{-1} = 1.46$  GHz, (c)  $f_{+1} = 3.12$  GHz.

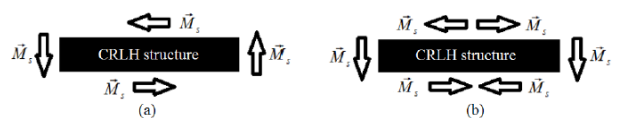


Fig. 9. Equivalent magnetic current density for: (a)  $f_0 = 2.1$  GHz, (b)  $f_{-1} = 1.46$  GHz and  $f_{+1} = 3.12$  GHz.

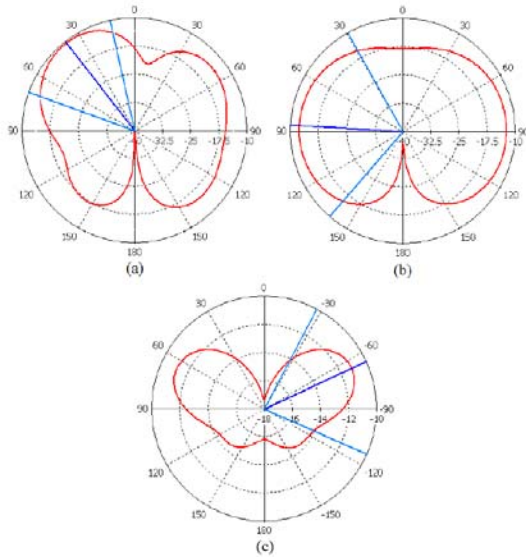


Fig. 10. Simulated radiation gain pattern at  $f_0 = 2.1$  GHz for: (a) different elevation angles and azimuth angle  $\varphi = 0^\circ$ , (b) different elevation angles and azimuth angle  $\varphi = 90^\circ$ , (c) different azimuth angles and elevation angle  $\theta = 90^\circ$ .

In the case of  $f_{-1} = 1.46$  GHz and  $f_{+1} = 3.12$  GHz resonance frequencies, in the points situated at the two ends of the resonator the electric field is  $180^\circ$  out of phase, corresponding to the distribution of a classical microstrip antenna operated at its first resonance frequency. Therefore, the equivalent magnetic current density along the length of the structure will cancel and only the two edges corresponding to the structure's width will be responsible for the radiation, producing a broadside radiation pattern, as shown in Fig. 11 and 12.

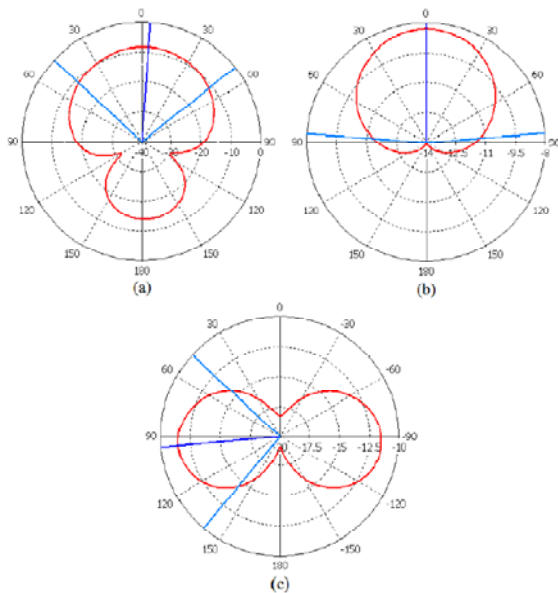


Fig. 11. Simulated radiation gain pattern at  $f_{+1} = 1.46$  GHz for: (a) different elevation angles and azimuth angle  $\varphi = 0^\circ$ , (b) different elevation angles and azimuth angle  $\varphi = 90^\circ$ , (c) different azimuth angles and elevation angle  $\theta = 90^\circ$

### 3. The series mode CRLH resonant antenna

Fig. 13 presents the proposed CRLH TL composed of four identical cells and terminated with a short-circuit. As shown in Fig. 14, at the zero order resonant frequency the input impedance of structure is very low, leading to a strong mismatch.



Fig. 13. The proposed series mode structure

In this case, the matching problem can be solved by integrating in the CRLH structure some elements designed on the basis of filter theory. At the zero order frequency, the short-circuited CRLH TL acts as a series mode resonator [1] and therefore by adding impedance K-inverters a first order band-pass filter topology can be obtained, as shown in Fig. 15.

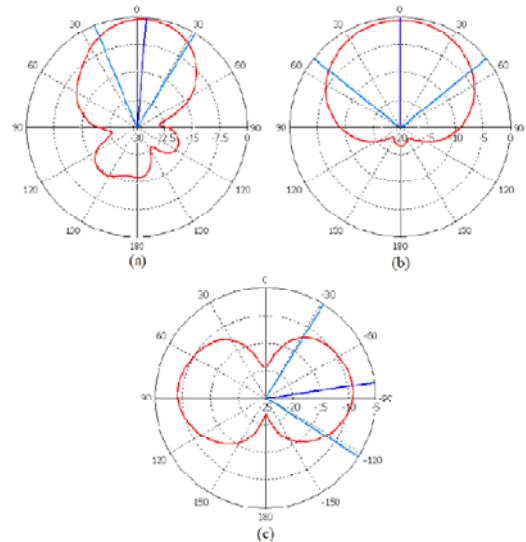


Fig. 12. Simulated radiation gain pattern at  $f_{+1} = 3.12$  GHz for: (a) different elevation angles and azimuth angle  $\varphi = 0^\circ$ , (b) different elevation angles and azimuth angle  $\varphi = 90^\circ$ , (c) different azimuth angles and elevation angle  $\theta = 90^\circ$ .

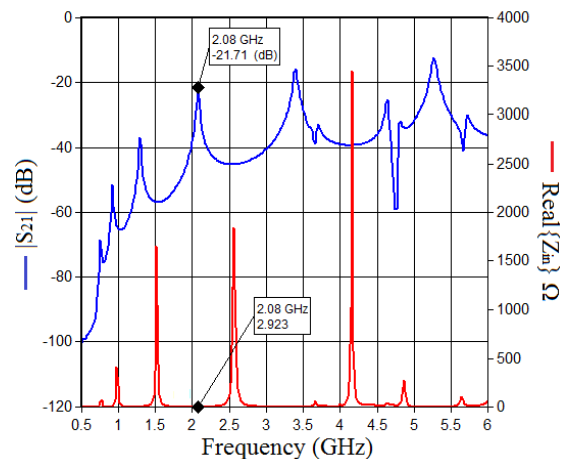


Fig. 14. Real part of input impedance

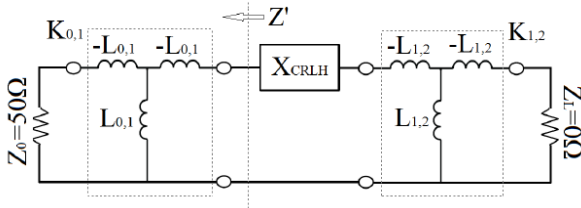


Fig. 15. Circuit model for first order band-pass filter.

When designing the band-pass filter from a low-pass prototype, the following design relation is applied [17]:

$$\frac{x_{CRLH}}{Z'} = \frac{g_0 g_1}{f_{BW}}, \quad (5)$$

where  $x_{CRLH}$  is the resonator's reactance slope parameter,  $g_0$  and  $g_1$  are the low-pass prototype parameters and  $f_{BW}$  is the fractional bandwidth of the band-pass filter.

Good matching to a common external network characterized by any impedance constant  $Z_0$  can be achieved if the inverter's inductance is obtained by using (6) which was derived from (5).

$$L_{0,1} = \frac{1}{2\pi f_0} \sqrt{\frac{x_{CRLH} Z_0 f_{BW}}{g_0 g_1}}. \quad (6)$$

Similarly  $L_{1,2}$  can be obtained, but its value will be zero, since the CRLH line is short-circuited.

Fig. 16 shows the geometry of the proposed CRLH series mode ZORA, matched to the external network by using the  $K_{0,1}$  impedance inverter.

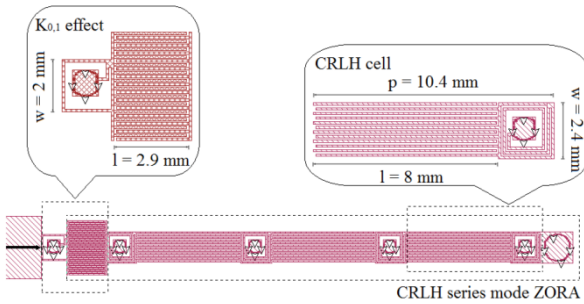


Fig. 16. CRLH series mode ZORA with four cells.

For this specific geometry the calculated reactance slope parameter is  $x_{CRLH} = 72.88 \Omega$  and its zero order frequency is  $f_0 = 2.1$  GHz. From (6), by specifying  $Z_0 = 50 \Omega$ ,  $f_{BW} = 4.28\%$  and  $g_0 = 1$ ,  $g_1 = 1.0178$ , where the latter two values are the parameters of a normalized first order Chebyshev filter with a ripple of 1 dB, we obtain the inverter's inductance  $L_{0,1} = 0.93$  nH.

While the parallel inductance value  $L_{0,1}$  is achieved by adding a short-circuited stub, the negative value series inductance  $-L_{0,1}$  is realized in practice by resorption, i.e. by properly decreasing the series inductance of the first interdigital capacitor. The impedance inverter's effect is obtained by only adding a small-sized, frequency

independent circuit.

As shown in Fig. 17, the matching is significantly improved at the frequency of 2.18 GHz, where the return loss reaches  $-31.85$  dB. At this frequency the antenna presents a broadside radiation pattern, as shown in Fig. 18, and has all its dimensions (including the matching circuit) independent of the operating frequency.

Table II presents the maximum obtained gain values for the proposed antennas at the resonant frequencies.

Table II. Simulated gain

Type	Frequency	Maximum gain (dB)
open-ended	$f_0 = 2.1$ GHz	-10.4 dB
open-ended	$f_{-1}^* = 1.46$ GHz	-8.3 dB
open-ended	$f_{+1}^* = 3.12$ GHz	-0.4 dB
short-circuited	$f_0 = 2.18$ GHz	0.1 dB

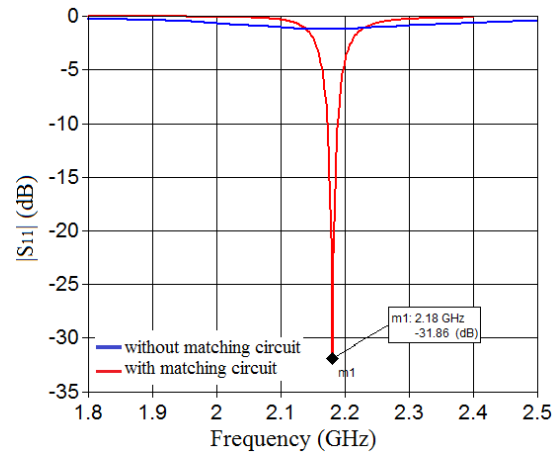


Fig. 17. Simulated  $|S_{11}|$  for the CRLH ZORA with and without matching circuit

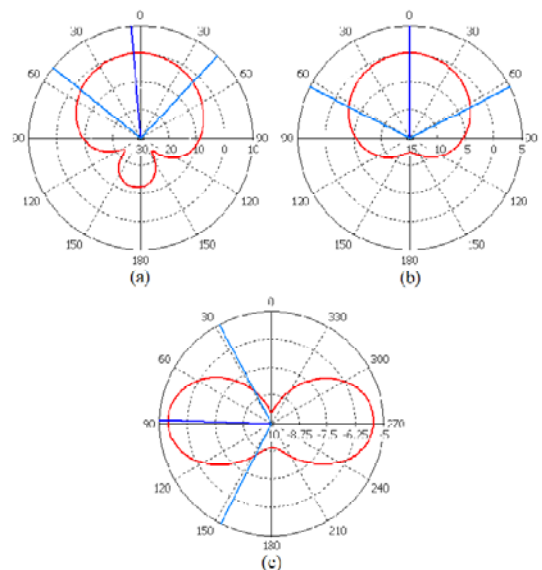


Fig. 18. Simulated radiation gain pattern for the antenna shown in Fig. 16 at  $f_0 = 2.18$  GHz for: (a) different elevation angles and azimuth angle  $\phi = 0^\circ$ , (b) different elevation angles and azimuth angle  $\phi = 90^\circ$ , (c) different azimuth angles and elevation angle  $\theta = 90^\circ$

## 5. Conclusions

Metamaterial CRLH TLs present new and unique properties that can be used in designing microwave devices with improved performances. Two such devices have been proposed and analyzed: the shunt mode resonant antenna and the series mode resonant antenna.

Due to the CRLH TL's dispersion diagram, the proposed antennas show multiple resonances. The resonance frequencies are not in harmonic ratios as in the case of regular resonators and they can be controlled by tailoring the dispersion diagram. The zero order resonance is of great interest due to the fact that it does not depend on the physical length of the resonator, allowing the design of miniaturized antennas.

In the case of the shunt mode resonant antenna, the matching problem has been solved by using a compact series inductor which cancelled the reactive part of the input impedance, in the vicinity of the resonant frequencies. Multiple operating bands have been achieved.

In the case of the series mode resonant antenna, the matching was obtained by integrating some classical filter theory elements in the design of the CRLH TL, achieving a miniaturized antenna with all its dimensions independent of the operating frequency.

The radiation characteristics have been also investigated. As expected, it shows different radiation patterns for the two modes and for the different resonant frequencies, in accordance with the electric field distributions. Having a relative low gain, the proposed antennas are suitable for short-range wireless communication systems.

## Acknowledgments

The work has been partially supported by the Romanian Ministry of Education and Research, project 72-230/2008 and by the Sectoral Operational Programme Human Resources Development 2007-2013 of the Romanian Ministry of Labour, Family and Social Protection through the Financial Agreement POSDRU/6/1.5/S/16.

## References

- [1] C. Caloz, T. Itoh, *Electromagnetic Metamaterials: Transmission Line Theory and Microwave Applications*, John Wiley & Sons, New Jersey (2006).
- [2] C. Wang, B.-J. Hu and X.-Y. Zhang, *IEEE Antennas and Wireless Propagation Letters*, **9** (2010).
- [3] J. K. Ji, G. H. Kim and W. M. Seong, *IEEE Antennas and Wireless Propagation Letters*, **8** (2009).
- [4] A. A. Fashi, M. Kamyab and M. Barati, *Progress In Electromagnetics Research C*, **14** (2010).
- [5] T. Jang, J. Choi, S. Lim, *IEEE Transactions on Antennas and Propagation*, **59** (2011).
- [6] S. Abielmona, H. V. Nguyen and C. Caloz, *IEEE Transactions on Antennas and Propagation*, **59** (2011).
- [7] P.-L. Chi, T. Itoh, *IEEE Transactions on Microwave Theory and Techniques*, **57** (2009).
- [8] M. Duran-Sindreu, G. Siso, J. Bonache and F. Martin, *IEEE Transactions on Microwave Theory and Techniques*, **58** (2010).
- [9] V. Gonzalez-Posadas, J. L. Jimenez-Martin, A. Parra-Cerrada, L.E. Garcia-Munoz and D. Segovia-Vargas, *IET Microwaves, Antennas & Propagation*, **4** (2010).
- [10] H. Choi, Y. Jeong, J. Lim, S.-Y. Eom and Y.-B. Jung, *IEEE Microwave and Wireless Components Letters*, **21** (2011).
- [11] A. Rennings, T. Liebig, C. Caloz and P. Waldow, *Proc. Asia-Pacific Microwave Conference, Bangkok, Thailand, 2007*, p. 191.
- [12] \*\*\*, Sonnet Software Inc., New-York.
- [13] M. A. Bueno, and A. K. T. Assis, *Journal of Physics D: Applied Physics*, **28** (1995).
- [14] C. A. Balanis, *Antenna Theory*, Wiley, New Jersey (1997).
- [15] A. Lai, K. M. K. H. Leong, and T. Itoh, *IEEE Transactions on Antennas and Propagation*, **55** (2007).
- [16] \*\*\*, CST Microwave Studio, CST – Computer Simulation Technology AG, Darmstadt (2011).
- [17] G. L. Matthaei, L. Young, E. M. T. Jones, *Microwave Filters, Impedance-Matching Networks, and Coupling Structures*, Artech House, New York (1980).

\*Corresponding author: ochetanaalexandru@yahoo.com